Effect of thermo-hydro-mechanical coupling on the evolution of stress in the concrete liner of an underground drift in the Cigéo project

IOP Conf. Series: Earth and Environmental Science **833** (2021) 012200 doi:10.1088/1755-1315/833/1/012200

Effect of thermo-hydro-mechanical coupling on the evolution of stress in the concrete liner of an underground drift in the Cigéo project

M Alonso[1], M N Vu[2], J Vaunat[1], G Armand[2], A Gens[1], C Plua[2], C De Lesquen[2] and O Ozanam[2]

[1]Universitat Politècnica de Catalunya, Barcelona, Spain
[2]French National Radioactive Waste Management Agency, Châtenay-Malabry, France

minh-ngoc.vu@andra.fr

Abstract. The French National Radioactive Waste Management Agency (Andra) is in charge of studying the disposal of high-level and intermediate-level long-lived waste (HLW and ILW-LL) in a deep geological repository (Cigéo project) within the host formation is the Callovo-Oxfordian claystone (COx). The heat emitted from waste packages induces a thermo-hydro-mechanical (THM) coupling within the structural elements and the host rock. This study focuses on the behavior of the concrete lining of an ILW-LL cell subjected to THM loading during its construction and operational phases. The mechanical behavior of the host rock is represented by an elasto-visco-plastic model taking into account the anisotropies in stiffness and strength. The coupled THM formulation is based on the Biot theory. Different simulations including full THM coupling and HM coupling with or without creep behavior of COx claystone have been performed to show the effect of the thermal load (generated by the waste packages), of the water seepage and of the creep strain of the host rock on the stress evolution in the concrete liner. The results show the preponderant role of the creep strain of COx claystone on the stress state of the liner during the operational phase, while the effect of the heat loading is moderate and that of the seepage is not significant.

1. Introduction

Within the context of deep geological radioactive waste disposal, the French National Radioactive Waste Management Agency (Andra) has been conducting a research program to demonstrate the feasibility of constructing and operating a High Level Waste (HLW) and Intermediate-Level Long-Lived (ILW-LL) disposal within the Callovo-Oxfordian (COx) claystone in the Meuse and Haute Marne departments, nearly 300 km East of Paris. This program includes scientific and technological in-situ experiments at the Meuse/Haute-Marne Underground Research Laboratory (MHM URL), laboratory tests on the sample scale, theoretical and numerical analysis. Numerous laboratory tests have been performed on the sample scale for 20 years to understand and characterize the hydromechanical behavior of COx claystone. Under a triaxial loading path, the instantaneous mechanical behavior of COx material exhibits the following main features: (a) linear elasticity under low deviatoric stress; (b) plastic hardening before the peak representing rather diffuse damage; (c) strain softening describing the post-peak behavior where macroracks are generally observed on the sample; (d) a residual stage controlled rather by the friction of macrocracks; (e) dependence of the mechanical response on the confining pressure with a transition from a brittle towards a ductile material (at confining stress about 20 MPa); (f) a slight

anisotropy in Young's modulus; and (g) a dependence of the compressive strength on the angle between the axial loading direction and the bedding plan [1]. Continuous monitoring has been also carried out at the MHM URL to understand the hydromechanical responses of COx claystone around drifts during and after their excavation. Particular attention has been made to the excavation induced damaged zone [2]; pore pressure distribution [3]; permeability change [4]; and rock deformation [5]. Moreover, COx claystone exhibits also time-dependent behavior, which is clearly observed by both laboratory tests and in-situ observation at the MHM URL [1]. Many constitutive models have been proposed, among which some models have successfully described several features of COx claystone at both sample and field scales, such as: local and non-local anisotropic elasto-visco-plastic models [6][7][8][9]; double phase field model [10]; etc.

The host formation in its natural state is saturated and has a low permeability (~ 10^{-20} m^2). The heat emitted from the exothermic waste packages leads to a temperature increase in the structure elements and in the host rock. This temperature increase triggers THM responses in the structure and the host rock including the thermal strain (or the thermomechanical stress) in materials and the increase in pore pressure in COx claystone due to the difference in thermal expansion coefficients between pore water and solid skeleton. The latter phenomenon has been evidenced by theoretical analysis [11][12]; laboratory tests [13]; and in-situ experiments at the MHM URL [14][15],[16].

The underground waste disposal will be divided into two main sections depending on the type of waste (ILW-LL or HLW) and the type of excavation method. The ILW-LL zone comprises tunnels of ~10 m in diameter (also referred as cells), which is planned to be excavated by TBM with an immediate installation of the liner. The liner of the ILW-LL cells consists of 0.5 m thick concrete tunnel lining segments covered by 0.2 m of compressible material. The compressible material exhibits a significant deformation (30-70%) under a low stress (0.5-2.0 MPa), which allows absorbing the time-dependent strains of the host rock and ensure the stability of the concrete liner during the operational phase (100-150 years).

This study focuses on assessing the stress evolution within the concrete liner of an ILW-LL cell of the Cigeo project by taking into account the main mechanical features of the host formation and the thermo-hydro-mechanical coupling under unsaturated condition. The COx claystone is described by the local anisotropic elasto-viscoplastic model proposed by Manica et al [6]. This model includes relevant features for a satisfactory description of the hydromechanical behavior of the argillaceous rock observed from both laboratory tests on sample scale and in-situ experiments at the MHM URL : nonlinear elasticity; nonlinear hardening plastic strain prior to peak strength; significant softening strain after peak; anisotropies in stiffness and strength; time-dependent viscoplastic strain and damage induced permeability increase. The stability of the ILW-LL tunnel is requested for the operational period (100-150 years), i.e. the concrete stress must not exceed the critical stress. Several simulations were carried out for different conditions: with and without thermal loading; with and without creep strain; which aims at evaluating the effects of the time-dependent behavior; of the thermal loading; and of the fluid seepage on the stress state of the concrete liner.

2. THM coupling

The fully coupled THM formulation used in this work were previously presented under unsaturated condition [17][18]. Figure 1 shows the principle of the full THM coupling for a porous rock with a low permeability like COx claystone. The THM formulation includes the mass balance equations for water and mineral species; the internal energy balance equation; and the balance momentum for a porous medium reducing to the equilibrium equation of macro stress; fluid flow obeys Darcy's law; heat transfer described by heat conduction (Fourier's law); heat convection; effective stress-strain relation given by a mechanical constitutive model; relations between suction, relative permeability and degree of saturation; as well as dependency of properties on THM variables (e.g. water properties versus temperature; permeability versus plastic deformation; etc). Details of these formulations can be found in [16][18].

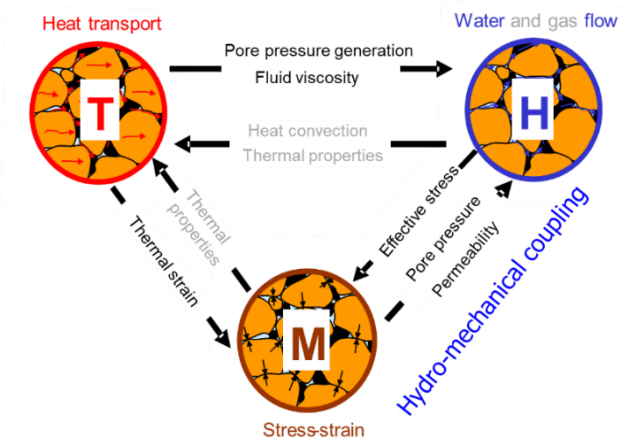

Figure 1. Principe of fully THM coupling in a porous medium of a low permeability (grey: not taking into or negligible).

3. Numerical model

3.1. Geometry model

A possible architecture of the Industrial Centre for Geological Disposal (Cigéo) is shown in Figure 2, which includes two area of surface facilities for nuclear activities and construction activities; ramps to transport waste packages from the surface to the main level of the disposal; shafts for construction/support activities, ventilation and transport of workers, and the main disposal. The main part of Cigéo is divided into two areas based on the waste types and the excavation size to emplace the waste packages: HWL zone (micro-tunnel of about 0.7-1.0 m in diameter) and ILW-LL one (tunnel of ~ 10 m in diameter).

As seen in Figure 2, the ILW-LL zone consists of several parallel tunnels. The length of the main part of an ILW-LL cell, where the waste packages are stored, is about ~500 m. Initial stress state is characterized by three principal stresses: vertical stress σ_v is close to the weight of the of the overburden; minor horizontal stress $\sigma_h \approx \sigma_v$; major horizontal stress $\sigma_H \approx 1.3\sigma_v$ within the COx layer. ILW-LL cells are planned to be excavated by TBM (with an intermediate installation of support) following the orientation of major horizontal stress. Obviously, the total heat power of waste packages, the chronology of package emplacement, and the depth are different from one cell to another. For sake of simplicity, an unfavourable case is considered where all the ILW-LL cells with an analogous depth are simultaneously filled by similar exothermic waste packages 4 years after the excavation. Thank to this assumption and the geometry configuration, 2D plane strain condition can be assumed, where only one cell is modelled in the geometry model and the interaction between cells is represented by the symmetrical condition.

As shown in Figure 3, a model representing the geological formations from the surface to 1000 m in depth is considered (a first layer from 0 to ~20 m is not modelled). The excavated diameter of the cell is D = 10.1 m and the distance between two adjacent cells is 5D, i.e. the larger of the model is 2.5D.

The support of the cell consists of a double layer: an inner concrete layer of 0.5 m covered by an outer compressible material layer of 0.2 m. In the real configuration of the ILW-LL cell, there is the secondary civil engineering for the operation of the cell, which is not considered in this study.

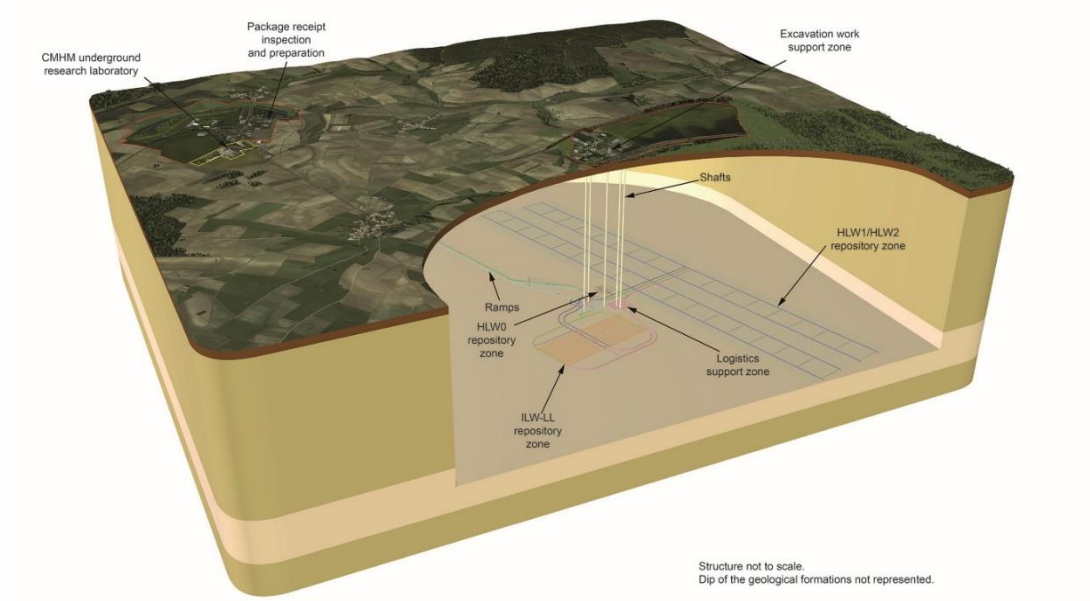

Figure 2. Possible architecture of the Cigéo project (for illustration).

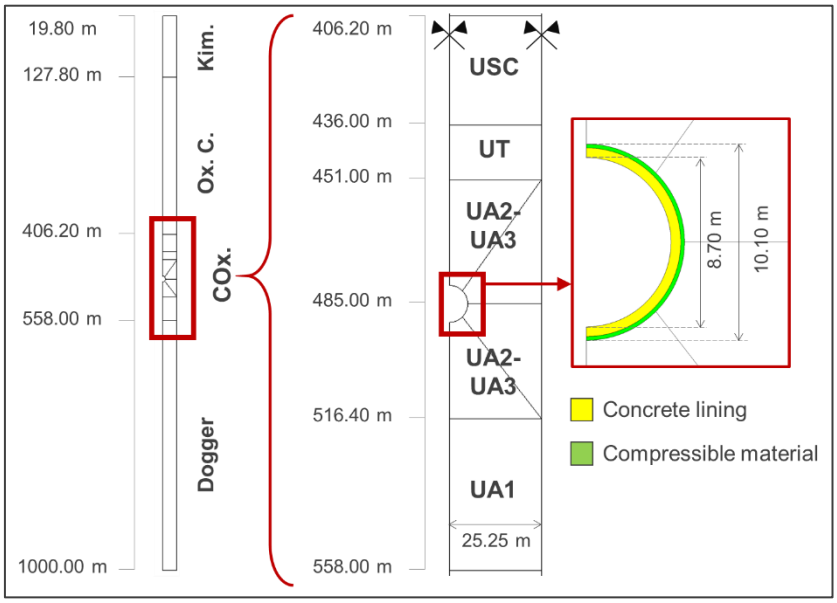

Figure 3. Geometry model.

3.2. Initial conditions

The temperature at the surface is assumed to be 8.7°C and the initial temperature as a function of depth is determined by the geothermal gradient of each layer as plotted in Figure 4a. The initial pore pressure is, in general, the hydrostatic water pressure. At the depth of the COx layer, an overpressure of 0.5 MPa has been observed in the MHM URL. This overpressure is modelled by a linear increase up to the cell depth and then it decreases to recover the hydrostatic pressure. The vertical stress σ_v is assumed to be the weight of the of the overburden and the minor horizontal stress is close to the vertical stress $\sigma_h \approx \sigma_v$. In the Kimmeridgian layer, the major horizontal stress $\sigma_H \approx \sigma_v$ and $\sigma_H \approx 1.3\sigma_v$ in the COx and Dogger layers. A linear interpolation of σ_H is made in the Oxfordian layer (Figure 5).

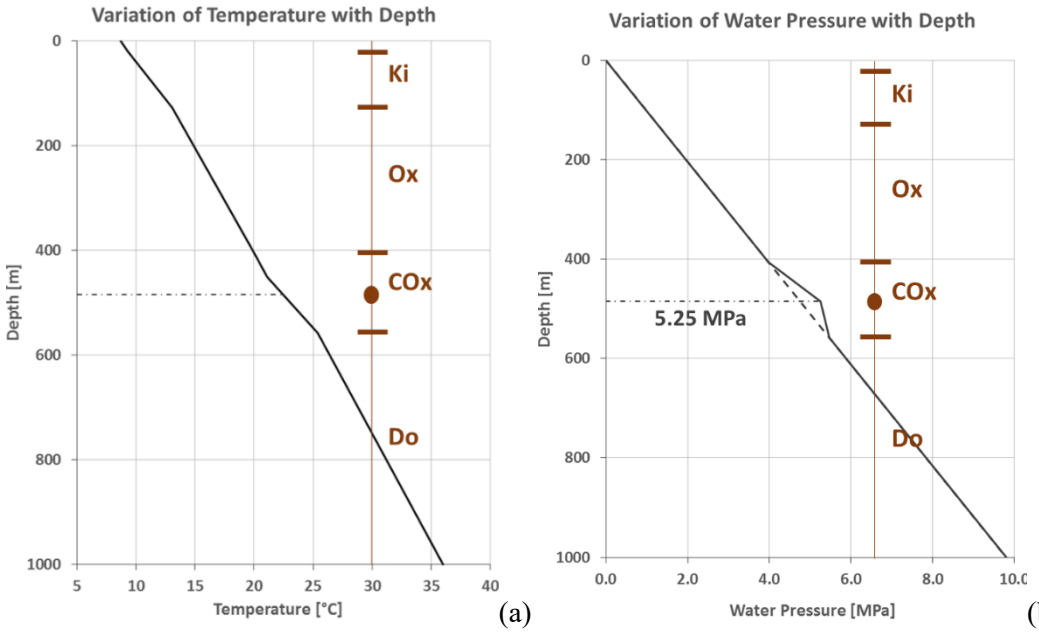

Figure 4. Initial temperature (a) and pore pressure (b).

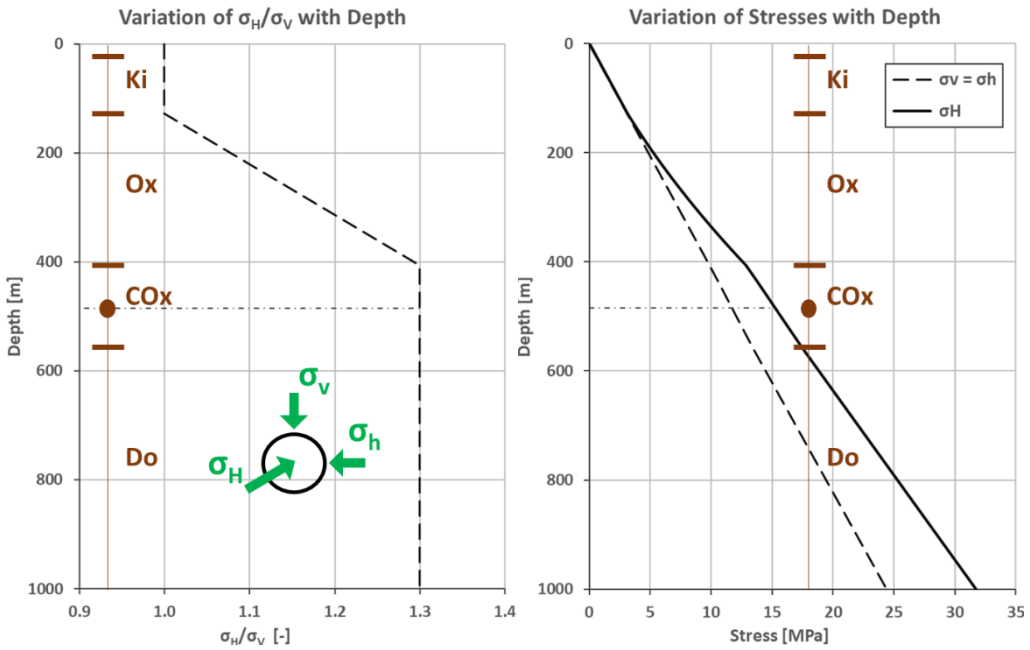

Figure 5. σ_H/σ_v ratio profile (left) and profiles of σ_H, σ_h, σ_v .

3.3. Boundary conditions and modelling phases

Initial total vertical stress, pore pressure and temperature are applied on the top surface. The right and left boundaries (without the cell wall) must verify the symmetrical condition (i.e. zero heat and fluid flow and nil horizontal displacement). On the bottom surface, the heat flow, the fluid flow and the vertical displacement are assumed to be zero. These boundary conditions are unchanged during the simulation of the ILW-LL cell.

Five modeling phases are simulated from the excavation of the ILW-LL cell to the end of operation period. The thermo-hydro-mechanical loading changes at the tunnel wall at each phase.

Phase N°0 is to apply the initial condition and to reach equilibrium of the system. At the excavation boundary, zero heat and fluid flow, as well as zero horizontal and vertical displacements are prescribed to reach equilibrium with the initial condition. The reaction (i.e. the force) on the excavation wall resulted from the equilibrium simulation will be used for the next phase.

Phase N°1 is the excavation of the ILW-LL cell. The excavation is simulated by the convergence-confining method represented by a confining ratio (CR). CR is the multiplication factor varying from 1 to 0, which describes the reduction in the reaction at the tunnel wall from phase N°0. During this phase, a linear reduction in CR from 1 to 0.04 during 0.5 days corresponding to a decrease from 100% to 4% of the initial reaction on the excavation boundary is assumed. The value of CR = 0.04 corresponds to the time of support installation. The water pressure is linearly reduced from the initial value to the suction s = 3.3 MPa corresponding to the relative humidity RH = 90% and initial temperature T = 22.5°C. Zero heat rate is still applied.

Phase N°2 corresponds to the installation of the support liners (concrete and compressible material layers). Finite elements representing the support are added into the model. Force applied on the excavation wall is removed and equilibrium between the support and the host rock is reached. A time lapse of 0.5 days is adopted. Suction s = 3.3 MPa and zero heat flow are prescribed on the inner boundary of the support.

Phase N°3 is the waiting phase. This is the time between the end of the tunnel construction and the beginning of the emplacement of the waste packages. The duration of this phrase is 4 years.

Phase N°4 is the operational phase that the heat release from the waste packages affects the THM behavior of the structural elements and the COx claystone. On the tunnel inner boundary, the water pressure is assumed to be zero, while the heat flow q_f given in Figure 6 is prescribed.

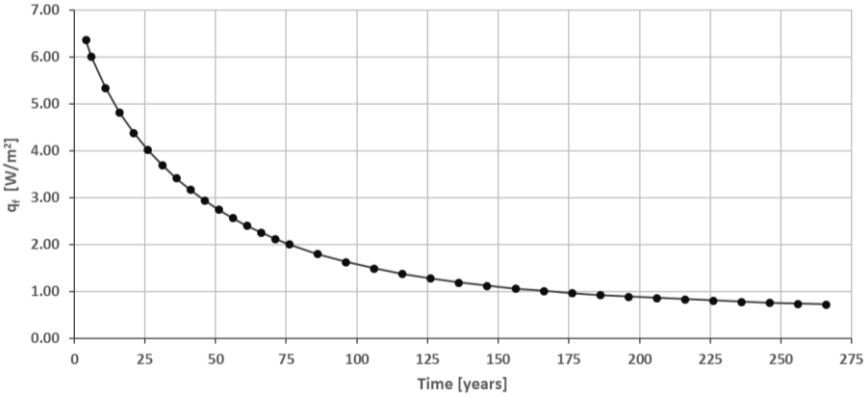

Figure 6. Time evolution of the heat flow applied at the tunnel inner wall.

3.4. Material behaviour and properties

All the formations except the COx claystone are assumed to behave elastically. The thermo-poro-elastic properties of each layer includes: five parameters of transversely elasticity; density; initial porosity; Biot coefficient; intrinsic permeability; thermal conductivity; specific heat; thermal expansion coefficient; parameters of the Van Genuchten law linking the suction and the degree of saturation; parameters of the generalized power law defining the relation between the relative permeability and the degree of saturation. Due to the limitation of the paper length, we do not give an exhaustive list of all these parameters for all the materials. However, the reader can refer to Plua et al. [19] to get an idea about THM parameters of these geological layers.

Short-term nonlinear and time-dependent behavior of COx formation is described by an anisotropic elasto-viscoplastic models. Details about this model and its parameters are found in Manica et al. [6] and Tourchi et al [16]. THM properties of water are also given by Tourchi et al [16].

The inner support layer is made from concrete of grade B60 (uniaxial compressive strength of 60 MPa). The behavior of the concrete liner is assumed to be elastic. The compressive material layer exhibits a high deformability (~50% corresponding under a low stress ~ 2-3 MPa). This material is

modelled by a trilinear elastic law. Its mechanical response under oedometric stress path and its parameters are shown in Figure 7. The deformation capacity of the compressible material helps to absorb the convergence of the excavation boundary due to the time-dependent response of the host rock, and thus to reduce the stress transmission to the concrete layer, as well as the concrete liner thickness. This is an innovative feature in the design of Cigéo project.

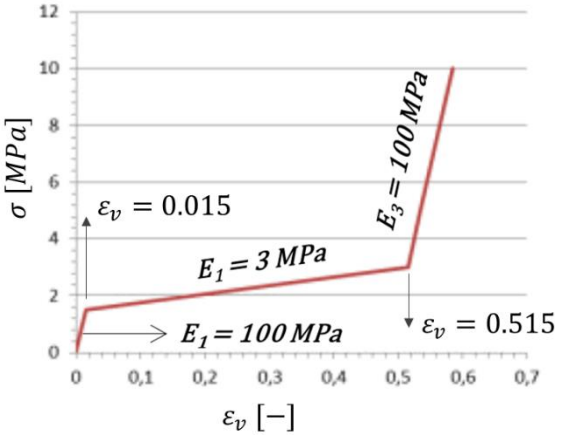

Figure 7. Mechanical response of the compressible material under the oedometric stress path.

4. Stress evolution in the concrete layer

Excavation leads to the redistribution of stress and pore pressure, which induces the creation of a damaged zone and the time-dependent responses of the host rock (convergence, water seepage, etc). The convergence of the excavation boundary is decelerated by the support system, even prevented if the support is rigid. This slow-down in convergence results in an increase of stress in the support. During phase N°3, the heat released from waste packages induces THM responses within the host rock and the support liner. This paper focuses only on the increase of stress in the concrete liner due to the time-dependent responses of host rock and thermal strain. Three simulations were performed to assess the effects of thermal load, creep strain and water flow: (1) elasto-plastic model with both creep strain and thermal load (EP-C-T) (i.e. reference case); (2) elasto-plastic model with creep strain but without thermal load (EP-C); and (3) elasto-plastic model without both creep strain and thermal load (EP). In the latter, the time-dependent response of COx claystone is essentially due to the water seepage. The evolution of maximal hoop stress within the concrete layer is shown in Figure 8 for these three cases.

As observed, the maximal stress in the concrete after 200 year is ~28 MPa lower than the accepted value (~34 MPa) for concrete B60 (60 MPa of compressive strength) according to Eurocode standard. Comparison between the three cases shows clearly a dominant effect of the host formation creep strain on the stress of the inner liner, while the effects of thermal load and of water seepage are not significant.

5. Conclusion

This work studies the THM modeling of an ILW-LL cell within the Cigéo project led by Andra in France, with a particular attention paid to the stress evolution within its concrete support. The host rock is modeled by a local anisotropic elasto-viscoplastic model, which includes many features: anisotropies in stiffness and strength; hardening, softening and residual strain; creep strain and damage induced permeability change. The result shows that the current design of the ILW-LL cell is robust since the maximal stress in the concrete liner at the end of the operational period is lower than its accepted value.

The increase in stress in the concrete liner is essentially controlled by the creep strain of the host formation, while the effects of the thermal load due to the heat release waste packages and of the water seepage due to the hydromechanical coupling are not significant compared to that of the rock creep strain.

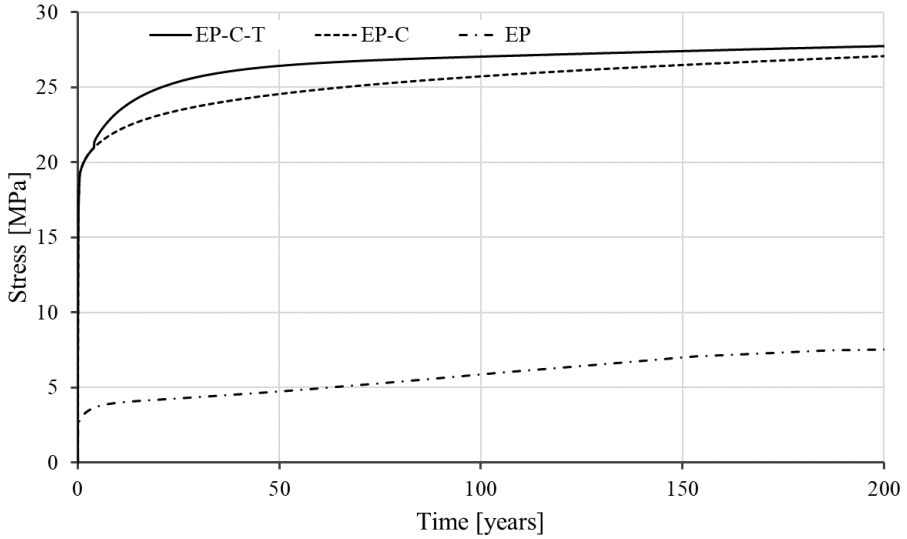

Figure 8. Evolution in maximal stress in concrete liner.

References

[1] Armand G, Conil N, Talandier J and Seyedi D 2017 *Comput Geotech* **85** 277-286
[2] Armand G, Leveau F, Nussbaum C, de La Vaissiere R, Noiret A, Jaeggi D, Landrein P and Righini C 2014 *Rock Mech Rock Eng* **47** 21–41
[3] Vu M N, Guayacán Carrillo L M and Armand G 2020 *Eur. J. Environ. Civ. Eng*. doi 10.1080/19648189.2020.1784800
[4] de La Vaissière R, Armand G and Talandier J 2015 J. Hydrol. **521** 141-156
[5] Armand G, Noiret A, Zghondi J and Seyedi DM 2013 *J Rock Mech Geotech Eng* **5** 221–30
[6] Manica M, Gens A, Vaunat J and Ruiz DF 2017 *Comput Geotech* **85** 341–350
[7] Pardoen B and Collin F 2017 *Comput Geotech* **85** 351-367
[8] Manica M, Gens A, Vaunat J, Armand G and Vu M N 2021 *Geotechnique* (accepted)
[9] Manica M, Gens A, Vaunat J, Armand G and Vu M N 2021 *Geotechnique* (accepted)
[10] Yu Z, Shao J, Vu M N and Armand G 2021 *Int. J. Rock Mech. Min. Sci.* **138** 104542
[11] Ghabezloo S and Sulem J 2009 *Rock Mech Rock Eng* **42** 1-24
[12] Vu M N, Armand G and Plua C 2020 *Rock Mech Rock Eng* **53** 2027–2031
[13] Mohajerani M, Delage P, Monfared M, Tang A M, Sulem J and Gatmiri B 2012 *Int. J. Rock Mech. Min. Sci.* **52** 112-121
[14] Bumbieler F, Plúa C, Tourchi S, Vu M N, Vaunat J, Gens A and Armand G 2021 *Int. J. Rock Mech. Min. Sci.* **137** 104555
[15] Conil N, Vitel M, Plua C, Vu M N, Seyedi D and Armand G 2020 *Rock Mech Rock Eng* **53** 2747-2769
[16] Tourchi S, Vaunat J, Gens A, Bumbieler F, Vu M N and Armand G 2021 *Comput Geotech* **133** 104045
[17] Olivella S, Gens A, Carrera J and Alonso E E 1996 Eng Comput 13 87–112
[18] Gens A, Vaunat J, Garitte B, Wileveau Y 2007 *Geotechnique* **57**(2) 207-228
[19] Plua C, Vu M N, Seyedi D and Armand G 2021 *Int. J. Rock Mech. Min. Sci.* (accepted)